

## Theory of Two-Magnon Raman Scattering in the Ordered Region for Cubic Antiferromagnets

U. Balucani

*Laboratorio di Elettronica Quantistica del Consiglio Nazionale delle Ricerche, 50127 Firenze, Italia*

V. Tognetti

*Istituto di Ricerca sulle Onde Elettromagnetiche del Consiglio Nazionale delle Ricerche, 50127 Firenze, Italia*

(Received 6 March 1973)

A Green's-function theory is applied to a study of two-magnon (2M) Raman scattering in cubic antiferromagnets in the ordered region. In addition to the first-order Hartree-Fock renormalization of the magnon energies together with 2M-interaction effects, a second-order theory gives additional contributions to the magnon self-energies. In particular, damping terms arising at this order are approximately evaluated for zone-boundary magnons, i.e., the ones relevant to the 2M Raman scattering process. Using a second-order expression for the 2M Raman cross section, this magnon damping is seen to eliminate the discrepancies of first-order theories. Quantitative comparison with experimental 2M Raman spectra gives a satisfactory agreement, both for the peak and the width of the spectra of  $\text{KNiF}_3$  and  $\text{RbMnF}_3$ , at least in the greatest part of the ordered region. The use of a simplified theory for the scattering cross section suggests the possibility of a simple estimation of zone-boundary magnon damping directly from experimental 2M spectra.

### I. INTRODUCTION

Two-magnon (2M) Raman scattering of light in various antiferromagnetic materials has been recently investigated in a number of papers,<sup>1-6</sup> with a satisfactory agreement between theory and experiment only at low temperatures. The main physical results of these investigations are: (i) Only near-zone-boundary (Z. B.) magnons are relevant to the scattering process, owing to the sharp peaking of the magnon density of states in this energy region; and (ii) it is necessary to consider the interaction between the two magnons due to the close proximity of the corresponding spin deviations in real space. At higher temperatures and even beyond the Néel point, experimental 2M Raman spectra<sup>7</sup> show a decrease of the peak frequency and of the over-all intensity of the spectrum with a marked increase of its width.

A spin-wave approach to the finite temperature spectra in the ordered region has been worked out by means of Bose operators, with a diagrammatic technique.<sup>2</sup> A first-order theory, using the equation of motion of the Green's functions, has been also performed.<sup>5</sup> Both treatments show that it is possible to quantitatively explain the downward shift of the Raman peak only with a Hartree-Fock renormalization of magnon energies. However, as discussed in Ref. 2, a first-order theory predicts increasing amplitudes and smaller widths of the spectrum at higher temperatures, in marked disagreement with experiments. Even if a more proper account of higher-order terms in the interaction between light and the magnetic system<sup>8</sup> improves the theoretical results somewhat, it is clear that

first-order theory cannot explain at all the shape (in particular, the width) of the 2M spectrum at higher temperatures. This rather negative statement is also confirmed by other first-order graphical approaches<sup>3,4</sup> which directly deal with spin operators, although it must be mentioned that these theories lead to a magnon-energy renormalization proportional to the sublattice magnetization, in disagreement with the persistence of the experimental 2M spectra above the Néel temperature  $T_N$ .

As we shall show later in detail, second-order theory consistently leads to additional terms in the magnon self-energies (second-order energy shift and damping). Graphically,<sup>2</sup> this corresponds to consider second-order diagrams for one-magnon propagators. Under the natural assumption that the main feature which determines the width of the Raman spectrum and its temperature variation is magnon damping, in Ref. 2 values of the latter quantity for Z. B. magnons have been phenomenologically fitted in order to give better agreement with experimental high-temperature spectra. However, it was difficult to justify these figures with a consistent calculation of Z. B. magnon damping: e.g., an estimate of this quantity<sup>2</sup> using a linear dispersion law led to values which are at best one order of magnitude lower than the fitted ones. Natoli and Ranninger<sup>6</sup> could justify the fitted value of the damping for  $\text{KNiF}_3$  at  $T = 0.7T_N$  in a semi-phenomenological way, i.e., using a scaling hypothesis on the experimental damping in  $\text{RbMnF}_3$  measured with inelastic neutron diffraction at various temperatures by Saunderson *et al.*<sup>9</sup>

The format of our paper is as follows. In Sec. II we review all first-order results for the inter-

acting magnon Hamiltonian and for the interaction between light and magnons. In Sec. III a second-order calculation of the 2M Green's function relevant for Stokes scattering is carried out. This leads to second-order magnon self-energies and to higher-order corrections for the 2M interaction. The imaginary part of the magnon self-energy leads to magnon damping. We evaluate the latter for Z. B. magnons in Sec. IV and Appendix B using various approximation schemes for the magnon density of states. Numerical values have been obtained for cubic antiferromagnets with the perovskite structure (KNiF<sub>3</sub>, RbMnF<sub>3</sub>). In Sec. V the Raman spectra at various temperatures in the ordered region are computed and successfully compared with experimental features of 2M spectra (peak frequency, width) in KNiF<sub>3</sub> and RbMnF<sub>3</sub>. Finally, a simple model is worked out which gives a satisfactory behavior of the Raman peak and width versus temperature.

## II. REVIEW OF FIRST-ORDER THEORY OF TWO-MAGNON RAMAN SCATTERING

We shall take in the following a model of an antiferromagnetic system describable in terms of a nearest-neighbor intersublattice exchange Heisenberg Hamiltonian

$$\mathcal{H} = J \sum_{\vec{j}} \sum_{\vec{\delta}} \vec{S}_{j,a} \cdot \vec{S}_{j+\vec{\delta},b}, \quad (1)$$

where the summation over  $\vec{j}$  runs over the  $N$  sites of sublattice  $a$  and the summation over  $\vec{\delta}$  runs over the  $z$  nearest neighbors of a given site. The presence of finite anisotropy terms does not alter most of our results; in any case, in cubic antiferromagnets, which we shall examine explicitly in the following (in particular, in RbMnF<sub>3</sub>), anisotropy terms are actually very small in comparison to exchange terms.

Let us perform on  $\mathcal{H}$  the usual Dyson-Maleev transformation to Bose operators. Fourier transforming the latter and diagonalizing the quadratic part of the Hamiltonian yields an interacting magnon Hamiltonian:

$$\mathcal{H} = \text{const} + \sum_{\vec{k}} \Omega_{\vec{k}} (\alpha_{\vec{k}}^\dagger \alpha_{\vec{k}} + \beta_{\vec{k}}^\dagger \beta_{\vec{k}}) + V, \quad (2)$$

with

$$V = -\frac{Jz}{N} \sum_{\vec{q}, \vec{q}', \vec{p}, \vec{p}'} \delta_{\vec{q}+\vec{p}-\vec{q}'-\vec{p}'} \times (I_{\vec{q}\vec{q}', \vec{p}\vec{p}'}^{\alpha\alpha} \alpha_{\vec{q}}^\dagger \alpha_{\vec{q}'}^\dagger \alpha_{\vec{p}} \alpha_{\vec{p}'} + I_{\vec{q}\vec{q}', \vec{p}\vec{p}'}^{\beta\beta} \beta_{\vec{q}}^\dagger \beta_{\vec{q}'}^\dagger \beta_{\vec{p}} \beta_{\vec{p}'} + I_{\vec{q}\vec{q}', \vec{p}\vec{p}'}^{\alpha\beta} \alpha_{\vec{q}}^\dagger \alpha_{\vec{q}'}^\dagger \beta_{\vec{p}}^\dagger \beta_{\vec{p}'}), \quad (3)$$

where  $\alpha_{\vec{k}}$ ,  $\beta_{\vec{k}}$  and  $\alpha_{\vec{k}}^\dagger$ ,  $\beta_{\vec{k}}^\dagger$  are magnon destruction and creation operators and

$$\Omega_{\vec{k}} = JSz(1 - \gamma_{\vec{k}}^2)^{1/2}, \quad (4)$$

$$I_{\vec{q}\vec{q}', \vec{p}\vec{p}'}^{\alpha\alpha} \equiv I_{\vec{q}\vec{q}', \vec{p}\vec{p}'}^{\beta\beta} = \gamma_{\vec{p}'-\vec{p}} u_{\vec{q}} u_{\vec{q}'} v_{\vec{p}} v_{\vec{p}'} + \frac{1}{2} \gamma_{\vec{q}} u_{\vec{q}} v_{\vec{q}'} v_{\vec{p}} v_{\vec{p}'} + \frac{1}{2} \gamma_{\vec{p}} u_{\vec{q}} u_{\vec{q}'} v_{\vec{p}} u_{\vec{p}'}, \quad (5)$$

$$I_{\vec{q}\vec{q}', \vec{p}\vec{p}'}^{\alpha\beta} = \gamma_{\vec{p}'-\vec{p}} u_{\vec{q}} u_{\vec{q}'} u_{\vec{p}} u_{\vec{p}'} + \gamma_{\vec{q}-\vec{q}'} v_{\vec{q}} v_{\vec{q}'} v_{\vec{p}} v_{\vec{p}'} + \gamma_{\vec{p}-\vec{p}'} u_{\vec{q}} v_{\vec{q}'} u_{\vec{p}} v_{\vec{p}'} + \gamma_{\vec{q}-\vec{q}'} v_{\vec{q}} u_{\vec{q}'} v_{\vec{p}} u_{\vec{p}'} + \gamma_{\vec{p}} (u_{\vec{q}} v_{\vec{q}'} u_{\vec{p}} u_{\vec{p}'} + v_{\vec{q}} u_{\vec{q}'} v_{\vec{p}} v_{\vec{p}'}) + \gamma_{\vec{p}'} (u_{\vec{q}} u_{\vec{q}'} u_{\vec{p}} v_{\vec{p}'} + v_{\vec{q}} v_{\vec{q}'} v_{\vec{p}} u_{\vec{p}'}), \quad (6)$$

with

$$u_{\vec{k}} = \left( \frac{1}{2(1 - \gamma_{\vec{k}}^2)^{1/2}} + \frac{1}{2} \right)^{1/2}, \quad (7)$$

$$v_{\vec{k}} = - \left( \frac{1}{2(1 - \gamma_{\vec{k}}^2)^{1/2}} - \frac{1}{2} \right)^{1/2}, \quad (8)$$

and

$$\gamma_{\vec{k}} = \frac{1}{z} \sum_{\vec{\delta}} e^{i\vec{k} \cdot \vec{\delta}} = \gamma_{-\vec{k}}. \quad (9)$$

In writing down Eqs. (2) and (3) we have implicitly made two approximations. First, we have neglected the so-called "Oguchi corrections", which arise in the normal ordering of  $V$ , i.e., the part of  $\mathcal{H}$  containing four operators. In three-dimensional cubic antiferromagnets that we will consider in the following, this amounts to neglecting a correction at most of 4% in the magnon energies. The second approximation consists of neglecting all the operators which have zero expectation values in the representation of noninteracting magnons.

This is exact in first-order theory (Hartree-Fock approximation) but corresponds to neglect possible "three-one" (confluence and splitting) damping mechanisms. Another approximation is to neglect every kinematical correction in the calculation of the average values of the physical quantities. Although the effect of kinematical interaction is not as clear in antiferromagnets as in ferromagnets, there is strong evidence from neutron inelastic scattering experiments that they are probably not important at least until  $0.95T_N$ . Thus in almost all the ordered region we can use an unrestricted boson representation of spin operators.

The simplest way to get a first-order renormalization of the magnon energies is to make a "mean-potential-energy" approximation in the last term of Eq. (3). This amounts to substituting for every product  $\alpha^\dagger \alpha$  and  $\beta^\dagger \beta$  its average value, to be self-consistently determined (Hartree-Fock approximation). For instance,

$$\alpha_{\vec{q}}^\dagger \alpha_{\vec{q}'} \beta_{\vec{p}}^\dagger \beta_{\vec{p}'} = \langle \alpha_{\vec{q}}^\dagger \alpha_{\vec{q}} \rangle \delta_{\vec{q}-\vec{q}'} \beta_{\vec{p}}^\dagger \beta_{\vec{p}'} + \langle \beta_{\vec{p}}^\dagger \beta_{\vec{p}'} \rangle \delta_{\vec{p}-\vec{p}'} \alpha_{\vec{q}}^\dagger \alpha_{\vec{q}'}. \quad (10)$$

Proceeding in this way we finally obtain after some algebra the Hartree-Fock temperature-dependent magnon frequencies

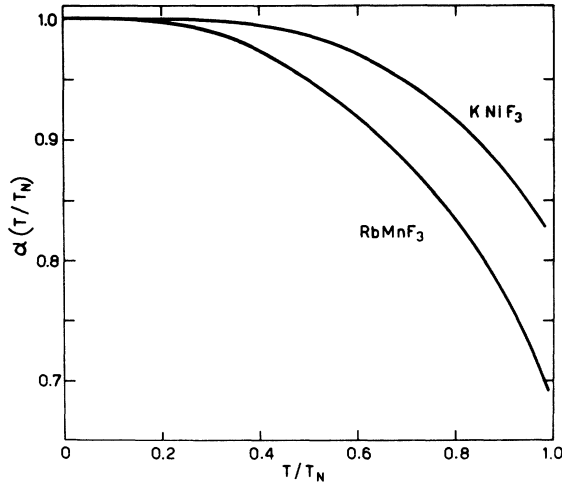


FIG. 1. Hartree-Fock renormalization factors for  $\text{KNiF}_3$  and  $\text{RbMnF}_3$  as a function of relative temperature  $T/T_N$ . The following values of the physical constants have been used: for  $\text{KNiF}_3$ ,  $J = 71 \text{ cm}^{-1}$ ,  $T_N = 253 \text{ }^\circ\text{K}$ ,  $S = 1$ ,  $z = 6$ ; for  $\text{RbMnF}_3$ ,  $J = 4.7 \text{ cm}^{-1}$ ,  $T_N = 82.6 \text{ }^\circ\text{K}$ ,  $S = \frac{5}{2}$ ,  $z = 6$ .

$$\bar{\Omega}_k = \alpha(T)\Omega_k, \quad (11)$$

where the Hartree-Fock renormalization factor is given by the implicit equation

$$\alpha(T) = 1 - \frac{1}{JzS^2} \frac{1}{N} \sum_q \Omega_q \langle \alpha_q^\dagger \alpha_q \rangle, \quad (12)$$

and

$$\langle \alpha_p^\dagger \alpha_p \rangle = \langle \beta_p^\dagger \beta_p \rangle = (e^{\alpha(T)\Omega_p/K_B T} - 1)^{-1}. \quad (13)$$

The renormalization factor  $\alpha(T)$  has been computed numerically by us for  $\text{KNiF}_3$  and  $\text{RbMnF}_3$  as a function of  $T/T_N$ , where  $T_N$  is the *experimental* Néel temperature. Results are plotted in Fig. 1 together with experimental data concerning these compounds.

Let us now consider explicitly the interaction between light and the magnetic system, which is responsible for 2M Raman scattering. It is generally assumed<sup>1,2</sup> that for the simple antiferromagnets which we are considering, this interaction can be

written as

$$M = \sum_j \sum_{\delta} \varphi_{\delta} \vec{S}_{j,a} \cdot \vec{S}_{j+\delta,b}, \quad (14)$$

where  $\varphi_{\delta}$  depends on the symmetry of the scattering mode and on the amplitudes and polarization vectors of the incident- and scattered-light electric fields. Introducing the Fourier transform

$$\Phi_k = \sum_{\delta} e^{i\vec{k}\cdot\delta} \varphi_{\delta} = \Phi_{-k}, \quad (15)$$

it is easily seen that in our antiferromagnets only the  $\Gamma_3^+$  mode is relevant for the scattering process, and for this mode  $\Phi_0 = \sum_{\delta} \varphi_{\delta} = 0$ . Let us now perform on  $M$  a Dyson-Maleev transformation to Bose operators, followed by a Fourier transform of the latter and a transformation on the quadratic part of  $M$ . This procedure is completely analogous to the one previously used for the system Hamiltonian  $\mathcal{H}$ , the only difference being the presence of  $\Phi_k$  instead of the Fourier transform of the exchange integral. Higher-order terms in  $M$  containing four Bose operators can be again treated in a Hartree-Fock approximation.<sup>8</sup> Focusing our attention only on the processes which involve either the creation or the destruction of two magnons, we finally have

$$M = \alpha(T)S \sum_{\vec{k}} \Phi_k (u_k^2 + v_k^2) (\alpha_k \beta_k + \alpha_k^\dagger \beta_k^\dagger). \quad (16)$$

A straightforward application of van Hove theorem gives for the scattering cross section an expression proportional to

$$K(\omega) = \frac{1}{1 - e^{-\omega/K_B T}} \lim_{\epsilon \rightarrow 0^+} \text{Im} \langle \langle M; M \rangle \rangle_{E=\omega+i\epsilon}, \quad (17)$$

where we have introduced the time Fourier transform  $\langle \langle M; M \rangle \rangle_E$  of the retarded Zubarev Green's function defined in the usual notation by

$$\langle \langle M(t); M \rangle \rangle = -i\theta(t) \langle [M(t), M] \rangle. \quad (18)$$

In Eq. (17)  $\text{Im}$  denotes the imaginary part and  $\omega$  is the frequency shift of the scattered light. If we limit ourselves to scattering processes which involve the creation of two magnons (Stokes scattering:  $\omega > 0$ ), substitution of Eq. (16) into Eq. (17) gives

$$\begin{aligned} K(\omega) &= \frac{1}{1 - e^{-\omega/K_B T}} \alpha^2(T) S^2 \lim_{\epsilon \rightarrow 0^+} \text{Im} \left\{ \sum_{\vec{k}, \vec{k}'} \Phi_k \Phi_{k'} (u_k^2 + v_k^2) (u_{k'}^2 + v_{k'}^2) \langle \langle \alpha_k \beta_k; \alpha_{k'}^\dagger \beta_{k'}^\dagger \rangle \rangle_{E=\omega+i\epsilon} \right\} \\ &= \frac{C}{1 - e^{-\omega/K_B T}} \alpha^2(T) S^2 \frac{1}{N} \lim_{\epsilon \rightarrow 0^+} \text{Im} \left\{ \sum_{\vec{k}, \vec{k}'} f_k f_{k'} (u_k^2 + v_k^2) (u_{k'}^2 + v_{k'}^2) \langle \langle \alpha_k \beta_k; \alpha_{k'}^\dagger \beta_{k'}^\dagger \rangle \rangle_{E=\omega+i\epsilon} \right\}, \end{aligned} \quad (19)$$

where, in the last member, we have introduced, following Ref. 2, the symmetrization factor  $f_k = (\cos k_x a - \cos k_y a)$  for the  $\Gamma_3^+$  mode. The constant  $C$  contains all the polarization dependence of this

scattering mode, together with the incident- and scattered-light electric fields.

The problem is now reduced to the calculation of the "two-particle" Green's function  $\langle \langle \alpha_k \beta_k; \alpha_{k'}^\dagger \beta_{k'}^\dagger \rangle \rangle_E$ .

As it is well known, writing down the equation of motion for this quantity introduces higher-order Green's functions, and an approximate solution can be obtained only with suitable decoupling procedures. As we will show in Appendix A, at least in the case of first- and second-order decouplings,

this procedure completely corresponds to summing up to infinite order classes of selected Feynman diagrams in an approach which uses one- and two-magnon propagators.<sup>2</sup>

The exact equation of motion for  $\langle\langle\alpha_k\beta_k; \alpha_k^\dagger\beta_k^\dagger\rangle\rangle_E$  has the form

$$(E - 2\Omega_k) \langle\langle\alpha_k\beta_k; \alpha_k^\dagger\beta_k^\dagger\rangle\rangle_E = \frac{1}{2\pi} (2\langle\alpha_k^\dagger\alpha_k\rangle + 1)\delta_{k-k'} + \left(-\frac{JZ}{N}\right) \sum_{\tilde{p}} I_{k\tilde{p}, \tilde{p}k}^{\alpha\beta} \langle\langle\alpha_{\tilde{p}}\beta_{\tilde{p}}; \alpha_{\tilde{p}}^\dagger\beta_{\tilde{p}}^\dagger\rangle\rangle_E \\ + \left(-\frac{JZ}{N}\right) \sum_{\tilde{q}, \tilde{p}, \tilde{p}'} \delta_{k+\tilde{p}-\tilde{q}-\tilde{p}'} \{ (I_{k\tilde{q}', \tilde{p}\tilde{p}'}^{\alpha\alpha} + I_{\tilde{p}\tilde{q}', k\tilde{p}'}^{\alpha\alpha}) \langle\langle\alpha_{\tilde{p}}^\dagger\alpha_{\tilde{q}'}\beta_{\tilde{p}}; \alpha_{\tilde{p}}^\dagger\beta_{\tilde{q}'}^\dagger\rangle\rangle_E \\ + (I_{\tilde{q}'\tilde{p}, \tilde{p}'\tilde{p}}^{\beta\beta} + I_{\tilde{q}'\tilde{p}, \tilde{p}'k}^{\beta\beta}) \langle\langle\alpha_k\beta_{\tilde{p}}^\dagger\beta_{\tilde{p}'}\beta_{\tilde{q}'}; \alpha_{\tilde{p}}^\dagger\beta_{\tilde{q}'}^\dagger\rangle\rangle_E \\ + I_{k\tilde{q}', \tilde{p}\tilde{p}'}^{\alpha\beta} \langle\langle\alpha_{\tilde{q}'}\beta_{\tilde{p}}^\dagger\beta_{\tilde{p}'}\beta_{\tilde{q}'}; \alpha_{\tilde{p}}^\dagger\beta_{\tilde{q}'}^\dagger\rangle\rangle_E + I_{\tilde{p}'\tilde{p}, \tilde{q}'k}^{\alpha\beta} \langle\langle\alpha_{\tilde{p}'}^\dagger\alpha_{\tilde{p}}\alpha_k\beta_{\tilde{q}'}; \alpha_{\tilde{p}}^\dagger\beta_{\tilde{q}'}^\dagger\rangle\rangle_E \}. \quad (20)$$

First-order theory decouples the higher-order Green's functions which appear in the curly brackets of Eq. (20) with a Hartree-Fock approximation similar to that already used in the renormalization of one-magnon energies. One obtains

$$(E - 2\bar{\Omega}_k) \langle\langle\alpha_k\beta_k; \alpha_k^\dagger\beta_k^\dagger\rangle\rangle_E = \frac{1}{2\pi} (2\hat{n}_k + 1)\delta_{k-k'} \\ + \left(-\frac{JZ}{N}\right) (2\hat{n}_k + 1) \sum_{\tilde{p}} I_{k\tilde{p}, \tilde{p}k}^{\alpha\beta} \langle\langle\alpha_{\tilde{p}}\beta_{\tilde{p}}; \alpha_{\tilde{p}}^\dagger\beta_{\tilde{p}}^\dagger\rangle\rangle_E, \quad (21)$$

where the statistical averages  $\hat{n}_k = \langle\alpha_k^\dagger\alpha_k\rangle$  are to be determined self-consistently according to Eqs. (12) and (13). The first-order-theory result expressed by Eq. (21) yields, of course, a Hartree-Fock renormalization of one-magnon energies ( $\Omega_k - \bar{\Omega}_k$ ). However, because we deal with a two-particle Green's function, we obtain also additional terms which take into account the interaction between the created magnons at first order. These terms are present even at  $T=0$  (where  $\hat{n}_k=0$ ), where they give the magnon-interaction effect first investigated by Elliott and Thorpe.<sup>1</sup>

Starting from Eq. (21) it is not difficult to obtain a closed expression for the quantity  $K(\omega)$ , which is proportional to the 2M Stokes cross section.<sup>5</sup> Some details of the calculations and of the connection with the diagrammatic approach are given in Appendix A. The final result becomes

$$K(\omega) = \frac{C}{1 - e^{-\omega/K_B T}} \alpha^2(T) S^2 \left(-\frac{1}{2\pi}\right) \\ \times \text{Im} \frac{L_2 + \frac{1}{2} J(L_1 L_1 - L_0 L_2)}{1 - \frac{1}{2} J(L_0 + L_2) - \frac{1}{4} J^2(L_1 L_1 - L_0 L_2)}, \quad (22)$$

where

$$L_m(E) = -\frac{1}{N} \sum_{\mathbf{k}} f_{\mathbf{k}}^2 (u_{\mathbf{k}}^2 + v_{\mathbf{k}}^2)^m \frac{2\hat{n}_{\mathbf{k}} + 1}{E - 2\bar{\Omega}_{\mathbf{k}}}. \quad (23)$$

Equation (22), which was first obtained in Ref. 2

with diagram techniques, can be further simplified if one notes that, owing to the sharp peaking of the magnon density of states in the zone-boundary region, a negligible error is made if we take  $u_{\mathbf{k}}^2 + v_{\mathbf{k}}^2 \sim 1$ . In this case  $L_0 \sim L_1 \sim L_2$  and we have

$$K(\omega) = \frac{C}{1 - e^{-\omega/K_B T}} \alpha^2(T) S^2 \left(-\frac{1}{2\pi}\right) \text{Im} \frac{L_0(E)}{1 - J L_0(E)}. \quad (24)$$

This completes the first-order-theory review in this section. While theoretical 2M spectra predicted by Eq. (24) are in good agreement with experiments for the temperature dependence of the Stokes peak, no agreement at all is obtained for the width of the spectrum. As a matter of fact, first-order theory gives widths that, *at best*, are essentially constant at increasing temperatures, while experimental spectra indicate a marked increase of these widths, which is particularly evident in the temperature range beyond  $0.5T_N$ . As we will show in Secs. III-V, these features can be accounted for only in a second-order theory, which considers also magnon damping.

### III. SECOND-ORDER THEORY

Second-order theory delays to a later stage any decoupling approximation of the infinite hierarchy for the equations of motion of the Green's function. While a formal correspondence with diagrammatic approaches remains also in this case, the calculations become very cumbersome. It what follows we shall omit all the unessential details.

Let us start from Eq. (20), which is exact, and let us write the equations of motion for all the higher-order Green's function in the curly brackets. Of course this introduces even more complicated Green's functions which, however, can be decoupled. For these we use a decoupling procedure introduced by Balcar<sup>10</sup> in the ferromagnetic case. To clarify this procedure, let us consider a particular higher-order Green's function appearing in

the right-hand side of Eq. (20), e.g., the first one  $\langle\langle\alpha_p^\dagger\alpha_{p'}\alpha_{q'}\beta_k; \alpha_k^\dagger\beta_k^\dagger\rangle\rangle_E$ . We can split it in diagonal and off-diagonal parts. The diagonal part has been considered in the first-order theory and corresponds to the decoupling

$$\langle\langle\alpha_p^\dagger\alpha_{p'}\alpha_{q'}\beta_k; \alpha_k^\dagger\beta_k^\dagger\rangle\rangle_E^{\text{diag}} \rightarrow \langle\alpha_p^\dagger\alpha_{p'}\rangle\langle\alpha_{q'}\beta_k; \alpha_k^\dagger\beta_k^\dagger\rangle_E + \delta_{q'-p}\langle\langle\alpha_{p'}\beta_k; \alpha_k^\dagger\beta_k^\dagger\rangle\rangle_E. \quad (25)$$

When we write down in second-order theory the exact equation of motion for the above-mentioned

Green's function, we need not bother to consider the information already contained in the diagonal part. The nondiagonal part gives (i) terms which renormalize the frequencies of the magnon modes into  $\langle\langle\alpha_p^\dagger\alpha_{p'}\alpha_{q'}\beta_k; \alpha_k^\dagger\beta_k^\dagger\rangle\rangle$ , (ii) terms which can be twice decoupled in order to give contributions proportional to  $\delta_{k+p-q'-p'}$ , and (iii) higher-order terms which can be neglected in this second-order approximation. After some tedious algebraic manipulations, the second-order approximation for this Green's function gives

$$\begin{aligned} (E + \bar{\Omega}_p - \bar{\Omega}_{p'} - \bar{\Omega}_{q'} - \bar{\Omega}_k) \langle\langle\alpha_p^\dagger\alpha_{p'}\alpha_{q'}\beta_k; \alpha_k^\dagger\beta_k^\dagger\rangle\rangle_E = & -\frac{JZ}{N} \delta_{k+p-p'-q'} (I_{p'k, q'p}^{\alpha\alpha} + I_{q'p, p'k}^{\alpha\alpha} + I_{q'p, p'p}^{\alpha\alpha} + I_{p'p, q'k}^{\alpha\alpha}) \\ & \times [\hat{n}_p(\hat{n}_{p'} + \hat{n}_{q'} + 1) - \hat{n}_{p'}\hat{n}_{q'}] \langle\langle\alpha_k\beta_k; \alpha_k^\dagger\beta_k^\dagger\rangle\rangle_E - \frac{JZ}{N} \delta_{k+p-p'-q'} \{I_{p'p, q'k}^{\alpha\beta} [\hat{n}_p(\hat{n}_{p'} + \hat{n}_k + 1) - \hat{n}_{p'}\hat{n}_k] \\ & \times \langle\langle\alpha_{q'}\beta_{q'}; \alpha_k^\dagger\beta_k^\dagger\rangle\rangle_E + I_{q'p, p'k}^{\alpha\beta} [\hat{n}_p(\hat{n}_{q'} + \hat{n}_k + 1) - \hat{n}_{q'}\hat{n}_k] \langle\langle\alpha_{p'}\beta_{p'}; \alpha_k^\dagger\beta_k^\dagger\rangle\rangle_E\}. \quad (26) \end{aligned}$$

If we introduce this result into Eq. (20) and compare with the first-order-theory [Eq. (21)], we easily recognize the first term in the right-hand side of Eq. (26) as one giving a second-order contribution to magnon self-energies, while the second term represents a higher-order correction to the Elliott-Thorpe interaction between the magnons. Treating, in a similar way, all the higher-order Green's functions appearing in Eq. (20) and substituting the results in the same equation, we finally obtain a second-order expression for the Green's function  $\langle\langle\alpha_k\beta_k; \alpha_k^\dagger\beta_k^\dagger\rangle\rangle_E$ :

$$\begin{aligned} [E - 2\bar{\Omega}_k - 2\Sigma_k'(E)] \langle\langle\alpha_k\beta_k; \alpha_k^\dagger\beta_k^\dagger\rangle\rangle_E = & \frac{1}{2\pi} (2\hat{n}_k + 1) \delta_{k-k} + \left(-\frac{JZ}{N}\right) (2\hat{n}_k + 1) \sum_{\vec{p}} I_{k\vec{p}, k\vec{p}}^{\alpha\beta} \langle\langle\alpha_{\vec{p}}\beta_{\vec{p}}; \alpha_k^\dagger\beta_k^\dagger\rangle\rangle_E \\ & + 2\left(\frac{JZ}{N}\right)^2 \sum_{\vec{q}, \vec{p}, \vec{p}'} \delta_{k+p-p'-q'} \left[ (I_{kq', p'p'}^{\alpha\alpha} + I_{p'p', kq'}^{\alpha\alpha} + I_{kp', p'q'}^{\alpha\alpha} + I_{p'q', kp'}^{\alpha\alpha}) I_{p'p', q'k}^{\alpha\beta} \right. \\ & \times \left( \frac{\hat{n}_p(\hat{n}_{p'} + \hat{n}_k + 1) - \hat{n}_{p'}\hat{n}_k}{E + \bar{\Omega}_p - \bar{\Omega}_{p'} - \bar{\Omega}_{q'} - \bar{\Omega}_k} + \frac{\hat{n}_{p'}(\hat{n}_p + \hat{n}_k + 1) - \hat{n}_p\hat{n}_k}{E + \bar{\Omega}_{p'} - \bar{\Omega}_p - \bar{\Omega}_{q'} - \bar{\Omega}_k} \right) \langle\langle\alpha_{q'}\beta_{q'}; \alpha_k^\dagger\beta_k^\dagger\rangle\rangle_E \\ & \left. + I_{kq', p'p'}^{\alpha\beta} I_{q'p', p'k}^{\alpha\beta} \frac{\hat{n}_{p'}(\hat{n}_{q'} + \hat{n}_k + 1) - \hat{n}_{q'}\hat{n}_k}{E + \bar{\Omega}_{p'} - \bar{\Omega}_p - \bar{\Omega}_{q'} - \bar{\Omega}_k} \langle\langle\alpha_{p'}\beta_{p'}; \alpha_k^\dagger\beta_k^\dagger\rangle\rangle_E \right], \quad (27) \end{aligned}$$

where the second-order contribution to the magnon self-energy is given by

$$\begin{aligned} \Sigma_k'(E) = & \left(\frac{JZ}{N}\right)^2 \sum_{\vec{q}, \vec{p}, \vec{p}'} \delta_{k+p-p'-q'} \left( \frac{\hat{n}_p(\hat{n}_{p'} + \hat{n}_{q'} + 1) - \hat{n}_{p'}\hat{n}_{q'}}{E + \bar{\Omega}_p - \bar{\Omega}_{p'} - \bar{\Omega}_{q'} - \bar{\Omega}_k} (I_{kq', p'p'}^{\alpha\alpha} + I_{p'q', kp'}^{\alpha\alpha}) \right. \\ & \left. \times (I_{p'k, q'p}^{\alpha\alpha} + I_{q'p, p'k}^{\alpha\alpha} + I_{q'p, p'p}^{\alpha\alpha} + I_{p'p, q'k}^{\alpha\alpha}) + \frac{\hat{n}_{p'}(\hat{n}_p + \hat{n}_{q'} + 1) - \hat{n}_p\hat{n}_{q'}}{E + \bar{\Omega}_{p'} - \bar{\Omega}_p - \bar{\Omega}_{q'} - \bar{\Omega}_k} I_{kq', p'p'}^{\alpha\beta} I_{q'p', p'k}^{\alpha\beta} \right). \quad (28) \end{aligned}$$

The  $E$  dependence of second-order self-energy causes the appearance of damping terms together with additional magnon energy shifts. In general, the latter lead to a  $\vec{k}$ -dependent renormalization factor. For temperatures not too close to  $T_N$ , the damping constant turns out to be practically constant in the Z. B. frequency region (see Appendix B). According to the Kramers-Kronig relations, the second-order energy shift in this region should be rather small. This conclusion is supported by the Raman-peak experimental data, which are in

good agreement with the first-order Hartree-Fock renormalization. Furthermore, for RbMnF<sub>3</sub> the neutron scattering data (Ref. 9) are consistent with a Z. B. magnon renormalization, which coincides within experimental errors with the Hartree-Fock renormalization, giving another evidence of the smallness of second-order shifts. Thus we shall focus our attention on damping terms, which surely must be essential in any explanation of the 2M spectra widths. An analytic continuation of  $\Sigma_k'(E)$  in the complex plane gives for these damping terms

(i. e., imaginary part of the self-energy) for  $\vec{k}$ -wave-vector magnons

$$\Gamma_{\vec{k}}(\bar{\Omega}_{\vec{k}}) = \pi \left( \frac{JZ}{N} \right)^2 \frac{1}{\hat{n}_{\vec{k}} + 1} \sum_{\vec{p}, \vec{r}} M(\vec{k}, \vec{p}', \vec{r}) \hat{n}_{\vec{p}'} (\hat{n}_{\vec{p}' - \vec{r}} + 1) \times (\hat{n}_{\vec{k} - \vec{r}} + 1) \delta(\bar{\Omega}_{\vec{k}} + \bar{\Omega}_{\vec{p}'} - \bar{\Omega}_{\vec{p}' - \vec{r}} - \bar{\Omega}_{\vec{k} - \vec{r}}), \quad (29)$$

where the momentum Kronecker  $\delta$  has been eliminated by introducing the momentum transfer  $\vec{r} = \vec{k} - \vec{q}' = \vec{p}' - \vec{p}$  and where we have replaced in the final result  $E$  with  $2\bar{\Omega}_{\vec{k}}$  (which again is consistent at not-too-high temperatures). In Eq. (29)  $M(\vec{k}, \vec{p}', \vec{r})$  is defined by

$$\begin{aligned} M(\vec{k}, \vec{p}', \vec{r}) &\equiv I_{\vec{k}(\vec{k}-\vec{r}), (\vec{p}'-\vec{r})\vec{p}'}^{\alpha\beta} I_{(\vec{k}-\vec{r})\vec{k}, \vec{p}'(\vec{p}'-\vec{r})}^{\alpha\beta} \\ &+ (I_{\vec{k}(\vec{k}-\vec{r}), -\vec{p}'(-\vec{p}'+\vec{r})}^{\alpha\alpha} + I_{-\vec{p}'(\vec{k}-\vec{r}), \vec{k}(-\vec{p}'+\vec{r})}^{\alpha\alpha}) \\ &\times (I_{(-\vec{p}'+\vec{r})\vec{k}, (\vec{k}-\vec{r})-\vec{p}'}^{\alpha\alpha} + I_{(\vec{k}-\vec{r})\vec{k}, (-\vec{p}'+\vec{r})-\vec{p}'}^{\alpha\alpha} \\ &+ I_{(\vec{k}-\vec{r})-\vec{p}', (-\vec{p}'+\vec{r})\vec{k}}^{\alpha\alpha} + I_{(-\vec{p}'+\vec{r})-\vec{p}', (\vec{k}-\vec{r})\vec{k}}^{\alpha\alpha}). \end{aligned} \quad (30)$$

As it stands, and within the above-mentioned approximations, Eq. (29) gives directly the damping constant for magnons with wave vector  $\vec{k}$  and renormalized Hartree-Fock energies  $\bar{\Omega}_{\vec{k}}$ . Similar expressions for  $\Gamma_{\vec{k}}(\bar{\Omega}_{\vec{k}})$  have been given in Refs. 2 and 11. However, only the damping behavior of small- $\vec{k}$  magnons has been analyzed in detail, while in the case of 2M Raman scattering the important contribution comes from near-zone-boundary magnons. Simple extrapolations of the small- $\vec{k}$  behavior have been tried<sup>2</sup> using an approximate linear dispersion law (and consequently a Debye-like density of states) but they give damping constants which are too small (at least one order of magnitude) for explaining the temperature behavior of the widths of 2M Raman spectra. In Sec. IV we shall give an approximate evaluation of  $\Gamma_{\vec{k}}$  for Z. B. magnons which seems to be more consistent and in better agreement with experimental data.

To conclude this section, let us return to Eqs. (27) and (28) which give the main result of second-order theory for 2M Stokes scattering. The presence of a second-order contribution to two-magnon interaction [last term in Eq. (27)] greatly complicates all further calculations and, in particular, it does not lead to a closed simple expression for the summation in Eq. (19). The physical effect of the last term in Eq. (27) is to give space- and time-dependent polarization effects which modify the simple "ladder" result  $1 - JL_0$  at the denominator of Eq. (24), possibly giving an effective  $(\vec{k}, E)$  dependence to the exchange integral. In order to keep the theory to a reasonable degree of mathematical simplicity, we shall neglect in the following the presence of this second-order contribution. It is difficult to give an accurate justification of this approximation: physically, perhaps, we may argue that in the temperature range considered

here, this approximation is not a bad one. Actually, any interaction between a single magnon and the entire bath of thermal-excited magnons becomes more likely than a more or less complicated interaction between the magnons created by the light electric field. This justification is partially supported by a flat-band calculation of this second-order effect, whose contribution turns out to be a factor  $1/z$  smaller than the second-order contribution to one-magnon self-energy. This result may suggest the possibility that also in the general case the neglected terms should become important only in the neighborhood of the critical region, but clearly here the entire spin-wave approach breaks down.

Therefore we are left with the simple second-order result

$$\begin{aligned} [E - 2\bar{\Omega}_{\vec{k}} - 2\Sigma_{\vec{k}}'(E)] \langle\langle \alpha_{\vec{k}} \beta_{\vec{k}}; \alpha_{\vec{k}'}^\dagger \beta_{\vec{k}'}^\dagger \rangle\rangle_E \\ = \frac{1}{2\pi} (2\hat{n}_{\vec{k}} + 1) \delta_{\vec{k}-\vec{k}'} + \left( -\frac{JZ}{N} \right) (2\hat{n}_{\vec{k}} + 1) \\ \times \sum_{\vec{p}} I_{\vec{k}\vec{p}, \vec{p}\vec{k}}^{\alpha\beta} \langle\langle \alpha_{\vec{p}} \beta_{\vec{p}}; \alpha_{\vec{k}'}^\dagger \beta_{\vec{k}'}^\dagger \rangle\rangle_E. \end{aligned} \quad (31)$$

It is clear that we obtain for the 2M Stokes cross section a result which is formally similar to Eq. (22) of first-order theory [or its simplified version, Eq. (24)] but with the new quantities

$$L_m(E) = -\frac{1}{N} \sum_{\vec{k}} f_{\vec{k}}^2 (u_{\vec{k}}^2 + v_{\vec{k}}^2)^m \frac{2\hat{n}_{\vec{k}} + 1}{E - 2\bar{\Omega}_{\vec{k}} - 2\Sigma_{\vec{k}}'(E)}, \quad (32)$$

which through the second-order self-energy part, directly contain magnon damping contributions to the 2M cross section.

#### IV. ZONE-BOUNDARY MAGNON DAMPING ESTIMATE

As in the first-order case, the  $\vec{k}$  summation in Eq. (32) strongly weighs zone-boundary magnons. Therefore we can evaluate one-magnon damping  $\Gamma_{\vec{k}}(\bar{\Omega}_{\vec{k}})$  as given by Eq. (29) only for magnons with  $\bar{\Omega}_{\vec{k}} \sim JSz$ .

At not-too-low temperatures, a small amount of anisotropy is sufficient to make thermal numbers of zone-boundary magnons not substantially different from the population of small-wave-vector modes. As the density of magnon states is sharply peaked in a narrow energy range near the Z. B. region, magnons in this region will be more effective in the damping process. Thus we can limit ourselves in Eq. (29) to consider only those modes  $\vec{p}'$  whose energy is sufficiently near to the zone-boundary value. On the other hand,  $\vec{k}$  magnons are just in this region, and the energy-conservation expressed by the  $\delta$  function can then be satisfied only if  $\vec{r}$  is such that also  $\bar{\Omega}_{\vec{p}' - \vec{r}}$  and  $\bar{\Omega}_{\vec{k} - \vec{r}}$  are in the Z. B. region. A slight error is then introduced if we take  $\hat{n}_{\vec{k}} \sim \hat{n}_{\vec{p}'} \sim \hat{n}_{\vec{k} - \vec{r}} \sim \hat{n}_{\vec{p}' - \vec{r}}$ . The complicated quantity  $M(\vec{k}, \vec{p}', \vec{r})$  which appears in Eqs. (29) and (30)

can now be evaluated in this limit, taking into account the definitions (5) and (6) and the fact that in the Z. B. region  $u \sim 1$ ,  $v \sim 0$ . The relative damping  $\Gamma(\Omega_k)/JSz$  of a magnon in the Z. B. energy region can therefore be approximated as

$$\frac{\Gamma(\Omega_k)_{Z.B.}}{JSz} \approx \frac{\pi}{S^2} \frac{\hat{n}_k(\hat{n}_k+1)}{\alpha(T)} \times \left[ \frac{1}{N^2} \sum_{\mathbf{r}} \gamma_r^2 \sum_{\mathbf{r}'} \delta(\epsilon_k + \epsilon_{\mathbf{r}'} - \epsilon_{\mathbf{r}'-\mathbf{r}} - \epsilon_{\mathbf{k}-\mathbf{r}}) \right], \quad (33)$$

where the reduced variable  $\epsilon_q = \Omega_q/JSz$  has been introduced.

In Appendix B we give an approximate evaluation of the numerical term in the square brackets in Eq. (33). The results of these calculations for the damping constant of a Z. B. magnon (with energy  $JSz$ ) are shown in Fig. 2 for  $\text{KNiF}_3$  and  $\text{RbMnF}_3$ . Qualitatively we can assert that these magnons are very-well-defined excitations, at least until temperatures of the order  $0.8T_N$ . In  $\text{RbMnF}_3$  neutron inelastic scattering data have been recently reported by Saunderson *et al.*<sup>9</sup> In particular, damping constants have been measured at various temperatures for magnons in the [001] direction. These experimental results for Z. B. magnons are plotted in Fig. 2. As mentioned in Ref. 9, the resolution power of the spectrometer introduces a systematic error which limits the accuracy of the measurements, especially at low temperatures where observed damping does not go to zero at  $T \rightarrow 0$ . However, we note that the over-all agreement with our theoretical estimates might not be as good as it appears: for instance, the Z. B. magnon energy in the [001] direction is slightly less than the maximum value  $JSz$ .

#### V. TWO-MAGNON RAMAN CROSS SECTION IN ANTIFERROMAGNETIC PEROVSKITES

If we take into account in the second-order expression for  $\langle\langle \alpha_k \beta_k; \alpha_k^\dagger \beta_k^\dagger \rangle\rangle_E$  [as given by Eqs. (27) and (28)] only the influence of one-magnon damping, we can easily obtain a closed expression for the quantity  $K(\omega)$  proportional to the 2M Stokes cross section. This expression is formally analogous to

$$\begin{aligned} L_0(\omega) &= - \int_0^{2JSz} dE \, 2E \frac{\coth[\alpha(T)E/4K_B T]}{\omega - \alpha E + i2\Gamma_k} \frac{1}{N} \sum_{\mathbf{k}} f_k^2 \delta(E^2 - 4\Omega_k^2) \\ &= - \frac{3}{\pi JSz} \int_0^1 dx \frac{x}{(1-x^2)^{1/2}} \frac{\coth[\frac{1}{2}(JSz/K_B T_N)\alpha(t)(x/t)]}{\omega/2JSz - \alpha(t)x + i\gamma'_k} \{C_{000}[3(1-x^2)^{1/2}] - C_{200}[3(1-x^2)^{1/2}] \\ &\quad + 2C_{110}[3(1-x^2)^{1/2}]\}, \quad (36) \end{aligned}$$

where  $\Gamma_k$  refers only to Z. B. magnons (again, a good approximation due to the sharp peaking of the

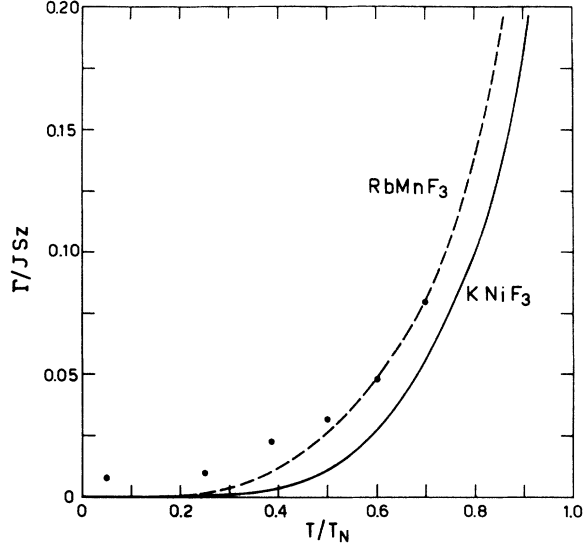


FIG. 2. Temperature dependence of relative zone-boundary magnon damping, as calculated by Eqs. (33) and (B2) for  $\text{KNiF}_3$  and  $\text{RbMnF}_3$ . Dots refer to the experimental values of the half-widths of zone-boundary magnons in the [001] direction, as reported for  $\text{RbMnF}_3$  in Ref. 9.

Eq. (22), with the only difference being that the quantities  $L_m(E)$  are now given by

$$L_m(E) = - \frac{1}{N} \sum_{\mathbf{k}} f_k^2 (u_k^2 + v_k^2)^m \frac{2\hat{n}_k + 1}{E - 2\Omega_k + i2\Gamma_k}. \quad (34)$$

Even here it is a good approximation to replace the quantities  $L_m(E)$  with  $L_0(E)$ , obtaining again Eq. (24). Evaluation of the imaginary part finally gives

$$\begin{aligned} K(\omega) &= \left( + \frac{1}{2\pi} \right) C JS^2 \left\{ \frac{\alpha^2(T)}{1 - e^{-\omega/K_B T}} \right. \\ &\quad \left. \times \frac{S(\omega)}{[1 - JR(\omega)]^2 + [JS(\omega)]^2} \right\}. \quad (35) \end{aligned}$$

Here  $R(\omega)$  and  $S(\omega)$  are the real and the imaginary part of  $L_0(\omega)$ , respectively. The last quantity can be put in the following form, which is more suitable for numerical calculations:

summation over the Brillouin zone). In the last member we have introduced reduced variables

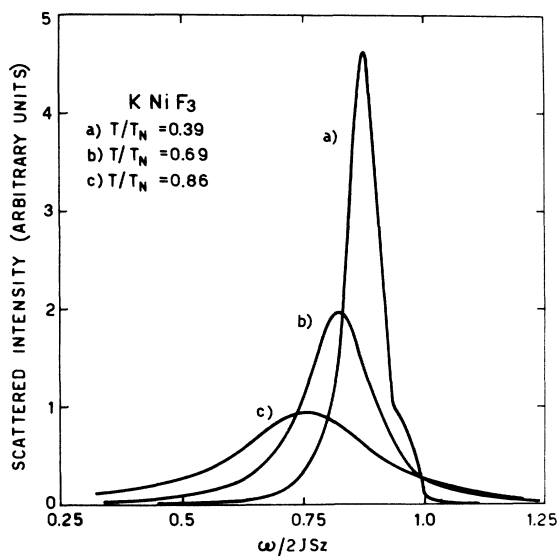


FIG. 3. Some computed two-magnon spectra in  $\text{KNiF}_3$  versus relative frequency at various temperatures.

$x = E/2JSz$ ,  $\gamma'_k = \Gamma_k/JSz$ , and  $t = T/T_N$ . The quantities  $C_{pqr}$  are defined by means of Bessel functions as

$$C_{pqr}(y) = \int_0^\infty d\tau \cos(y\tau) J_p(\tau) J_q(\tau) J_r(\tau), \quad (37)$$

and have been calculated and reported by many authors.<sup>12</sup>

We have calculated the expression in curly brackets in Eq. (35), which is proportional to the 2M Stokes cross section, in the case of  $\text{KNiF}_3$  and  $\text{RbMnF}_3$ . These computed spectra are presented in Figs. 3 and 4, using the estimated values of

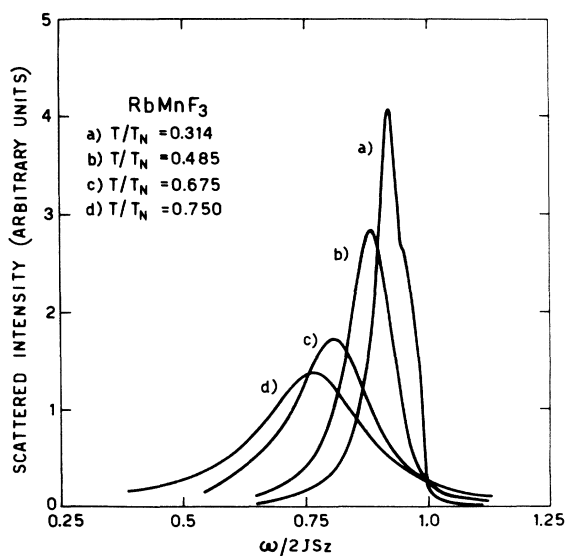


FIG. 4. Some computed two-magnon spectra in  $\text{RbMnF}_3$  versus relative frequency at various temperatures.

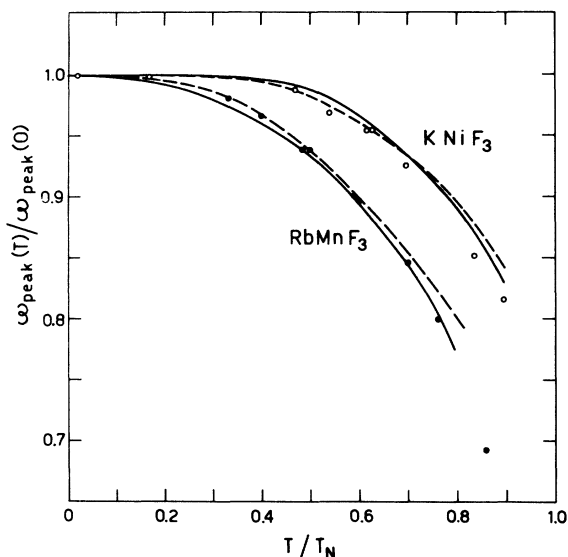


FIG. 5. Theoretical and experimental peak positions of two-magnon spectra as a function of temperature in  $\text{KNiF}_3$  and  $\text{RbMnF}_3$ . Here and in the following figures, the full curves have been obtained by a direct numerical evaluation of Eq. (36), whereas the dashed curves refer to the simplified model mentioned at the end of Sec. V. The experimental data for  $\text{KNiF}_3$  and  $\text{RbMnF}_3$  are taken from Refs. 2 and 13, respectively.

damping for zone-boundary magnons. The temperature variation of the relative peak frequency and of the full width at half-maximum of the spectra are plotted in Figs. 5-7 (solid line) together with the available experimental data for  $\text{KNiF}_3$ <sup>2</sup> and  $\text{RbMnF}_3$ .<sup>13</sup>

The comparison between theoretical and experimental peak frequencies (in terms of the zero-temperature peak frequency) gives a fair agree-

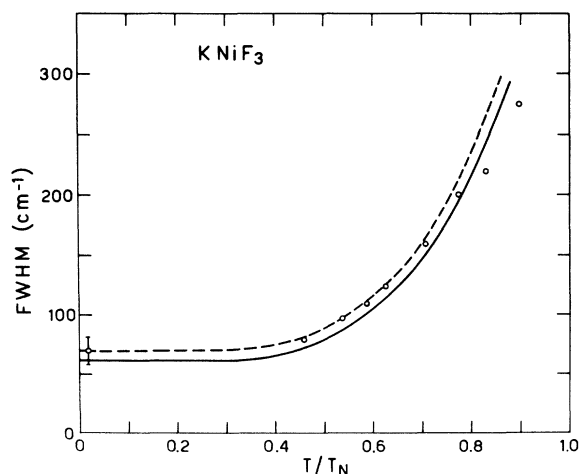


FIG. 6. Theoretical and experimental full widths at half-maximum of the two-magnon spectrum in  $\text{KNiF}_3$  as a function of temperature.



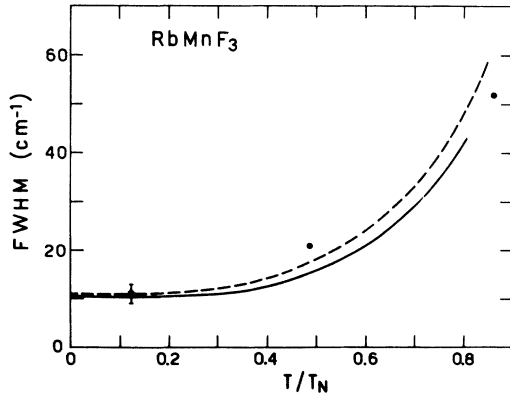


FIG. 7. Theoretical and experimental full widths at half-maximum of the two-magnon spectrum in  $\text{RbMnF}_3$  as a function of temperature.

ment, particularly in the case of  $\text{RbMnF}_3$  in most of the ordered region. As we stated before, this supports the physical assumption that Hartree-Fock renormalization of one-magnon energies is the main factor responsible for the decreasing of the 2M peak frequencies with increasing temperatures. Magnon "ladder" interactions further slightly decrease the peak frequencies by the presence of the factor  $2\hat{n}_k + 1$  in the corresponding term in Eq. (31). Figures 6 and 7 show a marked increase of the calculated full widths at half-maximum (solid line) of 2M spectra beyond  $T \sim 0.5T_N$ . This is essentially due to the introduction of one-magnon damping. In the case of  $\text{KNiF}_3$  the over-all comparison between theory and available experimental data is satisfactory, with some discrepancies as  $T \rightarrow T_N$ ,

probably due to our approximations in the calculation of zone-boundary magnon damping. The few published experimental data for the full width at half-maximum in  $\text{RbMnF}_3$  do not evidently allow a meaningful comparison, although a gross similarity of the temperature increase of the full width can be noted.<sup>14</sup>

The dashed lines in Figs. 5-7 are the result of a simplified semiphenomenological theory whose essential points are the following. At zero temperature an Ising flat-band approximation predicts a 2M Raman peak at a frequency  $2JSz - J$  (of course with a  $\delta$ -function-shaped spectrum). Even if this model may be not too bad owing to the sharp peaking of the density of magnon states in the Z. B. region, actual 2M spectra comprise a band of magnon frequencies in this region. Then, at  $T=0$ , a reasonable approximation for the 2M spectra of Heisenberg-type antiferromagnets may consist in taking an average magnon frequency  $\langle \Omega \rangle$  in this energy range and an effective bandwidth  $\Delta$  chosen in such a way to reproduce (after having allowed for magnon interactions) both the  $T=0$  experimental data for the peak and the full width at half-maximum of the 2M Raman spectrum. Clearly, in this fitting procedure we lose any minor structure of the spectrum (e.g., any slope discontinuities due to critical points in the Brillouin zone). After these assumptions, it is now possible to obtain a simple analytical solution for the 2M Stokes cross section at finite temperatures, taking into account that  $(1/N) \times \sum_{\mathbf{k}} f_{\mathbf{k}}^2 = 1$  for  $\Gamma_3^+$  scattering, and introducing magnon damping  $\Gamma_{\text{Z.B.}}$ , calculated in the same way as before. The final result is a scattering cross section proportional to

$$K'(\omega) = \frac{\alpha^2(T)}{1 - e^{-\omega/K_B T}} (2\langle \bar{n} \rangle + 1) \frac{\alpha(T)\Delta + 2\Gamma_{\text{Z.B.}}}{\left\{ \omega - [2\alpha(T)\langle \Omega \rangle - J(2\langle \bar{n} \rangle + 1)] \right\}^2 + \left\{ \alpha(T)\Delta + 2\Gamma_{\text{Z.B.}} \right\}^2}, \quad (38)$$

where  $\bar{n}$  is the magnon population at  $\langle \Omega \rangle$ , i.e., a Lorentz-shaped spectrum peaked at a frequency

$$\omega_{\text{peak}}(T) = 2\langle \Omega \rangle \alpha(T) - J(2\langle \bar{n} \rangle + 1), \quad (39)$$

with a full width at half-maximum (FWHM) given by

$$W_{\text{FWHM}}(T) = 2\alpha(T)\Delta + 4\Gamma_{\text{Z.B.}}. \quad (40)$$

Equations (39) and (40) are represented (dashed lines) in Figs. 5-7 after having fitted  $\omega_{\text{peak}}(0)$  and  $\Delta$  to the experimental values for  $\text{KNiF}_3$  and  $\text{RbMnF}_3$  at zero temperature. It can be seen that the results do not differ very much from the "exact" computed values and from most of the experimental data, thus confirming the essential validity of this simple model over most of the ordered region. In this temperature range Eqs. (39) and (40) may give

directly, in a 2M Raman scattering experiment, reasonable order of magnitude values for zone-boundary magnon damping.

## VI. CONCLUSION

In this paper we have employed the equation-of-motion method of the retarded Green's functions in order to calculate the two-magnon Raman scattering for a Heisenberg antiferromagnet at temperatures below  $T_N$ . The first-order decoupling, which takes into account the "ladder" interaction between magnons, gives a satisfactory description of the behavior of the Raman peak for cubic structures, like  $\text{KNiF}_3$  and  $\text{RbMnF}_3$ .

In order to calculate the width of the Raman spectrum, we have delayed to the second order the

decoupling in the Green's-function hierarchy, retaining only the terms which give the one-magnon lifetime. With some approximations we have estimated the Z. B. damping and we have computed the Raman spectrum, determining the peak position and the full width at half-maximum. The good agreement between theoretical values and experimental data shows that at low temperatures (as far as  $T \sim 0.5 T_N$ ) the width of the Raman spectrum is caused by band and "ladder" effects, while for higher temperatures the finite lifetime of the magnons is the most important reason of the broadening of the Raman spectrum.

Finally, we have derived an approximate expression for the Raman spectrum which gives the behavior of the peak and the width in agreement with the experimental data. We suggest that, using this expression, it is possible to obtain directly, with a 2M Raman experiment, reasonable order-of-magnitude values for zone-boundary magnon damping.

#### ACKNOWLEDGMENTS

We thank F. Barocchi for useful discussions at the beginning of this work. One of us (U. B.) wishes to thank the staff of the International Center of Theoretical Physics, Trieste for a stay during which part of this work has been performed.

#### APPENDIX A

For the sake of simplicity we put

$$g(E) \equiv \frac{C}{N} \sum_{\vec{k}, \vec{k}'} f_k f_{k'} (u_k^2 + v_k^2)(u_{k'}^2 + v_{k'}^2) G_{kk'}(E), \quad (\text{A1})$$

$$G_{kk'}(E) \equiv \langle \langle \alpha_k \beta_k; \alpha_{k'}^\dagger \beta_{k'}^\dagger \rangle \rangle_E,$$

and we write again the first-order equation (21) as

$$(E - 2\bar{\Omega}_k) G_{kk'} = \frac{1}{2\pi} (2\hat{n}_k + 1) \delta_{k-k'} + \left( -\frac{J_Z}{N} \right) (2\hat{n}_k + 1) \sum_{\vec{p}} I_{kp, pk}^{\alpha\beta} G_{pk'}. \quad (\text{A2})$$

With the definition

$$\Lambda_k(E) \equiv 2\pi \frac{E - 2\bar{\Omega}_k}{2\hat{n}_k + 1} \sum_{\vec{k}'} f_{k'} (u_{k'}^2 + v_{k'}^2) G_{kk'}(E), \quad (\text{A3})$$

Eqs. (A1) and (A2) can be written

$$g(E) = \frac{1}{2\pi} \frac{C}{N} \sum_{\vec{k}} f_k (u_k^2 + v_k^2) \frac{2\hat{n}_k + 1}{E - 2\bar{\Omega}_k} \Lambda_k(E), \quad (\text{A4})$$

$$\Lambda_k(E) = f_k (u_k^2 + v_k^2) + \left( -\frac{J_Z}{N} \right) \sum_{\vec{p}} I_{kp, pk}^{\alpha\beta} \frac{2\hat{n}_p + 1}{E - 2\bar{\Omega}_p} \Lambda_p(E). \quad (\text{A5})$$

These equations correspond to Eqs. (52) and (54) of Ref. 2 in a first-order theory, i. e., to a Bethe-Salpeter and vertex equations in a ladder approximation. Therefore, at least at this level of

approximation, there is a formal equivalence between the diagrammatic and equation-of-motion approaches. Taking into account the definition of  $I_{kp, pk}$  and the symmetry properties of the coefficients  $\gamma_k$  and  $f_k$ , it is possible to derive Eq. (22) with some lengthy algebraic calculations.

Equations (A4) and (A5) are, of course, no longer valid in a second-order theory, as it is easily shown comparing Eqs. (27) and (A2). However, if we neglect the last term in Eq. (27), which is responsible for higher-order 2M interactions, we arrive at equations formally analogous to (A4) and (A5), the only difference being that instead of Hartree-Fock one-magnon frequencies we have magnon second-order self-energies. Graphically,<sup>2</sup> this procedure would correspond to take two-particle Green's functions, in which one-magnon Hartree-Fock propagators are dressed with second-order diagrams easily recognizable from Eq. (28).

#### APPENDIX B

Here we give an approximate evaluation of the square-bracketed term in the damping expression of Eq. (33). We approximate the relative density of states by two rectangles. The first rectangle [amplitude  $\rho_1$ , energy interval  $(0, y)$ ] corresponds to low- and intermediate-energy magnons, while the second one [amplitude  $\rho_2$ , energy interval  $(y, 1)$ ] refers to magnons in a suitably defined "zone-boundary region." The parameters  $\rho_1$ ,  $\rho_2$ , and  $y$  can be separately determined by the three conditions:

$$\begin{aligned} \int_0^1 \rho(\epsilon) d\epsilon &= \rho_1 y + \rho_2 (1 - y) = 1, \\ \bar{\epsilon} &\equiv \frac{1}{N} \sum_{\vec{q}} \epsilon_q = \int_0^1 \epsilon \rho(\epsilon) d\epsilon = \rho_1 \frac{1}{2} y^2 + \rho_2 \frac{1}{2} (1 - y^2), \\ P &\equiv \frac{1}{N} \sum_{\vec{q}} \gamma_q^2 = \int_0^1 (1 - \epsilon^2) \rho(\epsilon) d\epsilon = 1 - \rho_1 \frac{1}{3} y^2 \\ &\quad - \rho_2 \frac{1}{3} (1 - y^3). \end{aligned} \quad (\text{B1})$$

The quantities  $\bar{\epsilon}$  and  $P$  can be exactly calculated and in the case of simple cubic antiferromagnets are 0.903 and  $\frac{1}{6}$ , respectively. Thus from Eqs. (B1) we obtain  $\rho_1 = 0.0856$ ,  $\rho_2 = 7.4$  and  $y = 0.875$ . The fact that  $\rho_2 \gg \rho_1$  indicates the sharp peaking of this approximate density of states in a narrow Z. B. region.

Let us now consider the square-bracketed term of Eq. (33) for the Z. B. magnon damping. The quantity  $1/N \sum_{\vec{p}} \delta(\epsilon_k + \epsilon_p - \epsilon_{p-r} - \epsilon_{k-r})$  can be approximated with the density of states  $\rho_2$  in the zone-boundary region  $(y, 1)$  because all the energies in the argument of the  $\delta$  function have been taken in this region. The remaining summation over  $\vec{r}$  is consequently restricted only to the modes such that  $\epsilon_{p-r}$  and  $\epsilon_{k-r}$  are in the Z. B. region. Most of

these modes correspond to low- $|\vec{\Gamma}|$  values or to low energies. Taking into account only these modes, this summation gives  $\rho_1(y - \frac{1}{3}y^3)$ . Substitution of numerical values finally yields

$$\frac{\Gamma_{Z,B_1}}{JS_Z} \sim 0.413 \frac{\pi \hat{n}_k(\hat{n}_k + 1)}{S^2 \alpha(T)}. \quad (B2)$$

Then the relative zone-boundary magnon damping can be also written ( $\epsilon_k = 1$ )

$$\frac{\Gamma_{Z,B_1}}{JS_Z} = 0.324 \frac{1}{S^2 \alpha(T)} \left[ \sinh \frac{\alpha(T) JS_Z}{2K_B T} \right]^{-2}, \quad (B3)$$

which is plotted in Fig. 2 for  $\text{KNiF}_3$  and  $\text{RbMnF}_3$ . In order to test the validity of our result we have estimated the square-bracketed term of Eq. (33) by using the relative exact density of states.<sup>12</sup>

Taking into account that the four frequencies in the  $\delta$  function are near the Z. B. energy region, we have

$$\begin{aligned} \frac{\Gamma_{Z,B_1}}{JS_Z} &= \frac{\pi \hat{n}_k(\hat{n}_k + 1)}{S^2 \alpha(T)} \\ &\times \left[ \left( \frac{6}{\pi} \right)^2 \int d\epsilon_r \epsilon_r (1 - \epsilon_r^2)^{1/2} C_{000} [3(1 - \epsilon_r^2)^{1/2}] \right. \\ &\times \left. \frac{\epsilon_{k-r}}{(1 - \epsilon_{k-r}^2)^{1/2}} C_{000} [3(1 - \epsilon_{k-r}^2)^{1/2}] \right], \quad (B4) \end{aligned}$$

where the integration should be performed on the values of  $\epsilon_r$  such that  $\epsilon_{k-r}$  is near the Z. B. energy region. Simple analytical approximations for  $\epsilon_{k-r}$  have given numerical values of the square-bracketed term of Eq. (B4), which have the same order of magnitude as the previous estimate.

<sup>1</sup>R. J. Elliott and M. F. Thorpe, *J. Phys. C* **2**, 1630 (1969).

<sup>2</sup>R. W. Davies, S. R. Chinn, and H. J. Zeiger, *Phys. Rev. B* **4**, 992 (1971); *Phys. Rev. B* **4**, 4017 (1971).

<sup>3</sup>J. Solyom, *Z. Phys.* **243**, 382 (1971); *Light Scattering in Solids*, edited by M. Balkanski (Flammarion, Paris, 1971), pp. 165-169.

<sup>4</sup>M. G. Cottam, *Solid State Commun.* **10**, 99 (1972); *J. Phys. C* **5**, 1461 (1972).

<sup>5</sup>U. Balucani, F. Barocchi, and V. Tognetti, *Phys. Lett. A* **40**, 339 (1972).

<sup>6</sup>C. R. Natoli and J. Ranninger, *Phys. Lett. A* **39**, 105 (1972); *J. Phys. C* **6**, 345 (1973).

<sup>7</sup>For a review of 2M Raman scattering experimental results, see P. A. Fleury, *Int. J. Magn.* **1**, 75 (1970).

<sup>8</sup>R. W. Davies, *Phys. Rev. B* **5**, 4598 (1972).

<sup>9</sup>D. H. Saunderson, C. G. Windsor, G. A. Briggs, M. T. Evans, and E. Hutchinson, in *IAEA Symposium on Neutron Inelastic Scattering*, Grenoble, 1972 (unpublished).

<sup>10</sup>E. Balcar, *J. Phys. C* **2**, 1174 (1969); *Acta Phys. Austriaca* **31**, 300 (1970).

<sup>11</sup>A. B. Harris, D. Kumar, B. I. Halperin, and P. C.

Hohenberg, *Phys. Rev. B* **3**, 961 (1971); E. Balcar, *J. Phys. (Paris)* **32**, 701 (1971).

<sup>12</sup>For example, T. Wolfram and J. Callaway, *Phys. Rev.* **130**, 2207 (1963); M. Yussouff and J. Mahanty, *Proc. Phys. Soc. Lond.* **85**, 1223 (1965). An error in the sign of  $C_{110}(y)$  in the interval 1.2 - 3 as tabulated in the last paper has been corrected.

<sup>13</sup>P. A. Fleury, *Phys. Rev. Lett.* **21**, 151 (1968); *J. Appl. Phys.* **41**, 886 (1970).

<sup>14</sup>It must be mentioned that for the highest temperatures in the ordered region, experimental spectra appear to have a less symmetrical shape than the theoretical ones (Figs. 3 and 4). Possibly, one may invoke a better treatment of the  $E$  dependence of the magnon self-energies or other higher-order effects (e.g., consideration of higher-order terms in the transition operator). However, in a spin-wave approach, surely such a program, apart from its complexity, will tend to obscure the reasonably simple physical representation of the 2M Raman process, which appears to give the dominant features to the spectra at least until  $T \simeq 0.8T_N$ .